

Itinerant-electron metamagnetism of $Y(\text{Co}, \text{Ni})_5$

This article has been downloaded from IOPscience. Please scroll down to see the full text article.

1999 J. Phys.: Condens. Matter 11 483

(<http://iopscience.iop.org/0953-8984/11/2/013>)

View [the table of contents for this issue](#), or go to the [journal homepage](#) for more

Download details:

IP Address: 171.66.16.210

The article was downloaded on 14/05/2010 at 18:28

Please note that [terms and conditions apply](#).

Itinerant-electron metamagnetism of $Y(\text{Co}, \text{Ni})_5$

H Yamada[†], K Terao[†], F Ishikawa[‡], M Yamaguchi[‡], H Mitamura[§] and T Goto[§]

[†] Faculty of Science, Shinshu University, Matsumoto 390-8621, Japan

[‡] Faculty of Engineering, Yokohama National University, Yokohama 240-8501, Japan

[§] Institute of Solid State Physics, The University of Tokyo, Tokyo 106-8666, Japan

Received 4 August 1998, in final form 22 September 1998

Abstract. Electronic structures of the pseudo-binary compound $Y(\text{Co}, \text{Ni})_5$ with the CaCu_5 -type hexagonal structure are calculated in the self-consistent linear muffin-tin orbital method within the atomic sphere approximation, by taking into account the preferential occupation sites for Ni. The calculated bulk moment disappears abruptly near 60% Ni concentration. Above the critical concentration of Ni, a metamagnetic transition from the paramagnetic to the ferromagnetic state is found to occur. These calculated results are consistent with the recently observed ones. It has been shown that the anomalous magnetic behaviours of $Y(\text{Co}, \text{Ni})_5$ can be explained by the detailed shape of the local density-of-states curve of the 3d-transition-metal atoms at the 3g site near the Fermi level.

1. Introduction

Intermetallic compounds of rare-earth and 3d-transition-metal atoms are known to show interesting magnetic properties associated with both localized moments of rare-earth atoms and itinerant electrons of 3d atoms [1]. In particular, the intrinsic magnetic properties of the 3d-rich intermetallics are discussed in the itinerant-electron model on the basis of the calculated electronic structures. For instance, ThCo_5 with the CaCu_5 -type hexagonal structure shows a metamagnetic transition (MT) from a state with a small magnetic moment to another one with a large moment at an applied magnetic field of about 8 T at low temperature [2]. Nordström *et al* [3] have calculated the electronic structure of ThCo_5 , and the MT is shown to be caused by the special shape of the density-of-states (DOS) curve near the Fermi level. Such a MT from a low-moment state (LMS) to a high-moment state (HMS) has also been observed for $\text{Ce}(\text{Co}, \text{Ni})_5$ [4].

Recently, the MT for $Y(\text{Co}_{1-x}\text{Ni}_x)_5$ with the same structure as ThCo_5 has been observed near the Ni concentration $x = 0.6$ [5]. The closed and open circles in figure 1 denote the observed magnetizations at 4.2 K without magnetic field and at the magnetic field $H = 40$ T, respectively. A large difference between the magnetizations at $H = 0$ and 40 T can be seen near $x = 0.6$. The aim of the present paper is to study theoretically the observed rapid increase of magnetization caused by the magnetic field near $x = 0.6$, by making use of the calculated electronic structures of $Y(\text{Co}, \text{Ni})_5$.

Calculations of the electronic structure of $Y\text{Co}_5$ have been carried out by many authors [6–10]. Co atoms in this compound occupy crystallographically different 2c and 3g sites. The local density of states (DOS) of a Co atom at a 2c site is very high at the Fermi level, so the strong ferromagnetic state is stabilized. On the other hand, a Co atom at a 3g site is shown to

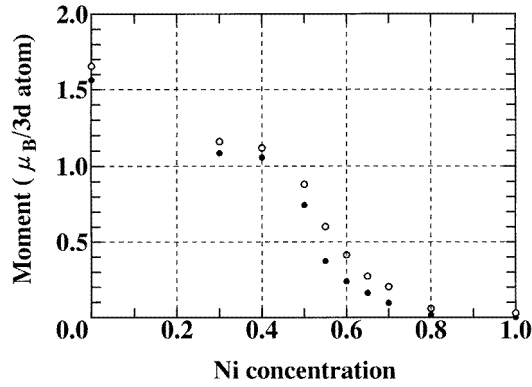


Figure 1. Observed magnetic moments of $Y(\text{Co}_{1-x}\text{Ni}_x)_5$ at 4.2 K. Closed and open circles represent those at $H = 0$ and 40 T.

have two magnetic states, the HMS and LMS, which are stabilized at larger and smaller lattice constants, respectively [9]. At the observed lattice constant of YCo_5 , the HMS of the 3g-site Co atom is stabilized by the effective exchange field of the 2c-site Co moments. However, the HMS of the 3g-site Co atom may become unstable when the 2c-site Co atoms are replaced by, say, Ni atoms. In fact, the Ni atoms in $Y(\text{Co}, \text{Ni})_5$ occupy predominantly 2c sites, rather than 3g sites [11, 12]. When the magnetically stable 2c-site Co atoms are replaced by nonmagnetic Ni atoms, the 3g-site Co atoms may change the HMS into the LMS at a certain concentration of Ni. Then, the MT from the LMS to the HMS occurs near the critical concentration of Ni.

In order to establish the validity of this prediction for the MT of $Y(\text{Co}, \text{Ni})_5$, the electronic structures of $Y(\text{Co}_{1-x}\text{Ni}_x)_5$ were calculated at $x \geq 0.4$, by a self-consistent linear-muffin-tin orbital (LMTO) method within the atomic sphere approximation (ASA), by taking into account the preferred site of Ni. Calculated results on the dependence of the magnetization on the Ni

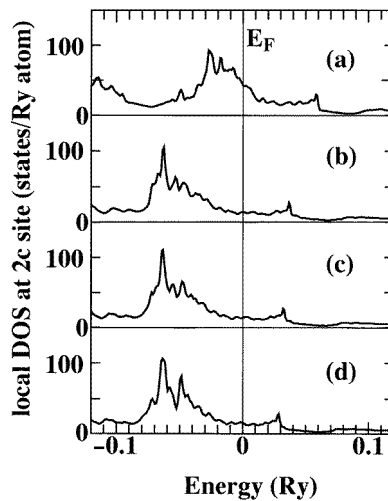


Figure 2. Calculated local DOSs (a) of the 2c-site Co in YCo_5 and (b), (c), (d) of the 2c-site Ni in $Y(\text{Co}_{1-x}\text{Ni}_x)_5$ for $x = 0.4, 0.5$ and 0.6 , respectively.

concentration are given in section 2. In section 3 the MT from the paramagnetic state to the ferromagnetic one is discussed, together with the results calculated by the fixed-spin-moment method. Our conclusions and a discussion are given in section 4.

2. Calculation of the electronic structure

We have recently obtained the dependence of the local moments on the lattice constant for YCo_5 , YCo_3Ni_2 and YNi_5 with CaCu_5 -type structure, by performing spin-polarized band calculations by the linear muffin-tin orbital (LMTO) method within the atomic sphere approximation (ASA) [9]. It has been found that the 3g-site Co atom has two magnetic states, the HMS and LMS, as mentioned in section 1. In this section the electronic structures of $\text{Y}(\text{Co}_{1-x}\text{Ni}_x)_5$ are calculated for $x = 0.4$ – 0.7 . We assume here that all of the 2c sites are occupied by Ni atoms at $x \geq 0.4$, as the preferred site of Ni is the 2c site [11, 12]. Although this assumption is a little far from the actual atomic arrangement in $\text{Y}(\text{Co}, \text{Ni})_5$, it is a useful model for studying the effect of the Ni atoms on the magnetic properties of $\text{Y}(\text{Co}, \text{Ni})_5$ when the Ni atoms at the preferred sites play an important role. The excess Ni atoms, as well as Co atoms, occupy the 3g site at $x > 0.4$. The numbers of Ni and Co atoms at the 3g site, in this model, are $5(x - 0.4)$ and $5(1 - x)$ in a unit cell, respectively. Furthermore, the 3g-site atom is treated as a virtual 3d atom with the averaged atomic number $5(x - 0.4)Z_{\text{Ni}}/3 + 5(1 - x)Z_{\text{Co}}/3$, where Z_{Ni} and Z_{Co} are the atomic numbers of Ni and Co.

The method of the calculation of the electronic structure is the same as in reference [9]. In the present paper, however, the irreducible $1/24$ Brillouin zone was sampled at 370 k -points to get the accuracy of the numerical calculations higher than that in reference [9]. Convergence in charge density was achieved such that the root mean square of the moment of the occupied partial density of states became smaller than 10^{-6} .

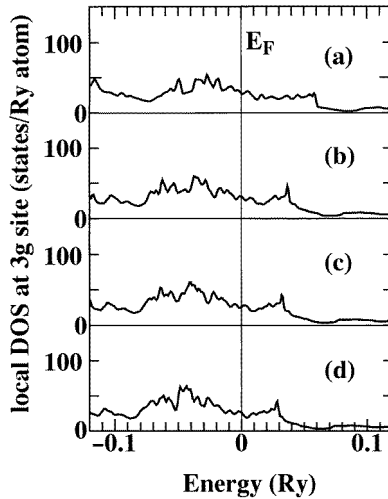


Figure 3. Calculated local DOSs (a) of the 3g-site Co in YCo_5 and (b), (c), (d) of the virtual 3d atom at the 3g site in $\text{Y}(\text{Co}_{1-x}\text{Ni}_x)_5$ for $x = 0.4, 0.5$ and 0.6 , respectively.

The calculated local DOS curves at the 2c and 3g sites are shown in figures 2 and 3, respectively, for $x = 0.0, 0.4, 0.5$ and 0.6 in $\text{Y}(\text{Co}_{1-x}\text{Ni}_x)_5$. Curves (a), (b), (c) and (d) in figure 2 are those of the 2c-site Co in YCo_5 , and of the 2c-site Ni for $x = 0.4, 0.5$ and 0.6 , respectively. Curves (a), (b), (c) and (d) in figure 3 denote the local DOS of the 3g-site Co

in YCo_5 , and of the virtual 3d atom of Co and Ni at the 3g site for $x = 0.4, 0.5$ and 0.6 , respectively. E_F denotes the Fermi level. As seen in figure 2(a), the position of E_F for YCo_5 lies rather close to the peak of the local DOS of the 2c-site Co. However, the position of E_F for $x \geq 0.4$ in $\text{Y}(\text{Co}_{1-x}\text{Ni}_x)_5$ is far from the peak of the local DOS. This is because the 2c site is occupied by Ni in these compounds. The height of the local DOS at E_F is small for $x \geq 0.4$, so the 2c-site Ni atom becomes nonmagnetic.

On the other hand, the position of E_F for YCo_5 is far from the broad peak of the local DOS of the 3g-site Co and the height of the local DOS at E_F is rather small. The positions of E_F for $x = 0.4, 0.5$ and 0.6 in $\text{Y}(\text{Co}_{1-x}\text{Ni}_x)_5$ shift toward the higher-energy side because the number of electrons of the virtual 3d atom increases with increasing x . Near $x = 0.6$, E_F lies near a broad minimum of the local DOS of the virtual 3d atom at the 3g site. This may be connected with the MT of $\text{Y}(\text{Co}_{1-x}\text{Ni}_x)_5$, as discussed in the following section.

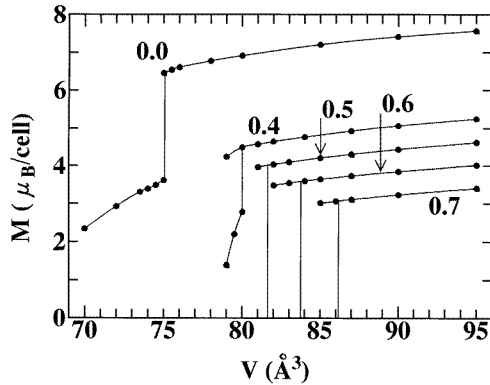


Figure 4. Calculated moments of $\text{Y}(\text{Co}_{1-x}\text{Ni}_x)_5$ as a function of the unit-cell volume V . The vertical lines denote the critical volumes V_C .

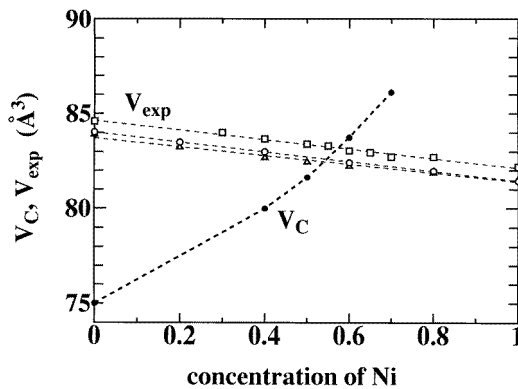


Figure 5. Calculated critical volumes V_C (closed circles) and the observed unit-cell volumes given in [5] (open squares), [11] (open triangles) and [14] (open circles).

The closed circles in figure 4 denote the calculated results for the bulk moment as a function of the unit-cell volume V where one Y and five Co or Ni atoms are included. The numbers shown on the curves denote the concentration x of Ni in $\text{Y}(\text{Co}_{1-x}\text{Ni}_x)_5$. It is seen that the two magnetic moments, large and small moments, are stabilized for $x = 0.0$ and 0.4 ,

depending on V . The vertical thin lines denote the critical volumes V_C , at which the energies of the two states are equal to each other. On the other hand, no small moment is stabilized for $x \geq 0.5$ and the paramagnetic state is stabilized at $V < V_C$.

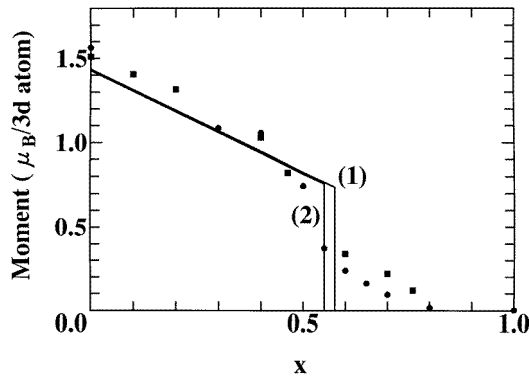


Figure 6. Concentration dependences of the magnetic moment, (1) and (2), calculated with the observed lattice constants given in [5] and [11], respectively. Closed circles and squares represent results observed at $H = 0$ given in [5] and [15].

The concentration dependence of V_C is shown by the closed circles in figure 5. The open squares, circles and triangles are observed values of V given in references [5], [11] and [13], respectively. Although there are some systematic differences between the observed values of V , the sudden decrease of the bulk moment of $Y(\text{Co}_{1-x}\text{Ni}_x)_5$ is shown to occur at $x = 0.55$ or 0.58 as shown in figure 6. The curves (1) and (2) in figure 6 are the results calculated with the lattice constants observed in references [5] and [11], respectively. The closed circles and squares are observed values given in [5] and [14]. A good agreement between the calculated and observed results is obtained except near the critical concentration. The difference near the critical concentration is attributable to the alloying effects—e.g., the local environment effect for the atoms—which are not taken into account in the present paper.

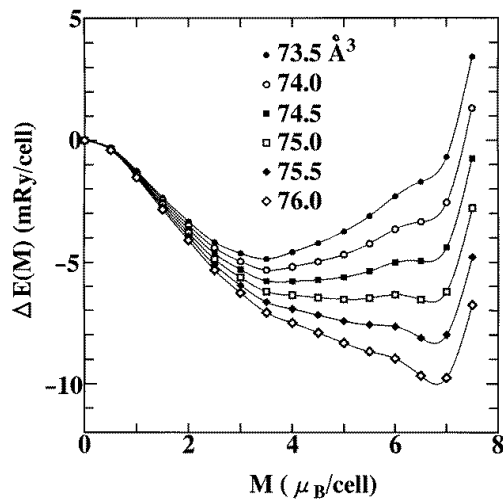


Figure 7. $\Delta E(M)$ calculated for YCo_5 at various unit-cell volumes.

3. Fixed-spin-moment calculation

The difference $\Delta E(M)$ between the energy at a given moment M and that at $M = 0$ is calculated by the fixed-spin-moment method [15]. Figure 7 shows $\Delta E(M)$ calculated for YCo_5 at various values of the unit-cell volume V . It can be seen that $\Delta E(M)$ has two minima at large and small values of M near the critical volume $V_C = 75.0 \text{ \AA}^3$. At larger volumes, the HMS with about $7 \mu_B/\text{cell}$ is stabilized. On the other hand, the LMS with about $3.5 \mu_B/\text{cell}$ is stabilized at smaller volumes. The minimum of $\Delta E(M)$ at large M is very sharp, while that at small M is rather broad. This means that the high-field susceptibilities for the HMS and LMS are small and large, respectively, because the second derivative of $\Delta E(M)$ with respect to M

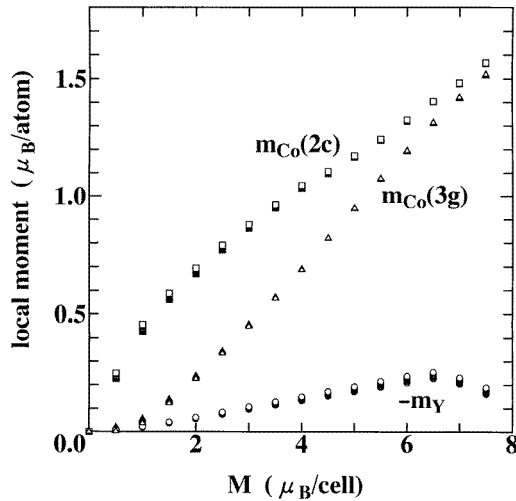


Figure 8. Calculated local moments $m_{\text{Co}(2c)}$, $m_{\text{Co}(3g)}$ and m_{Y} of the 2c-site Co, the 3g-site Co and the Y atoms in YCo_5 , respectively, as functions of the total moment M .

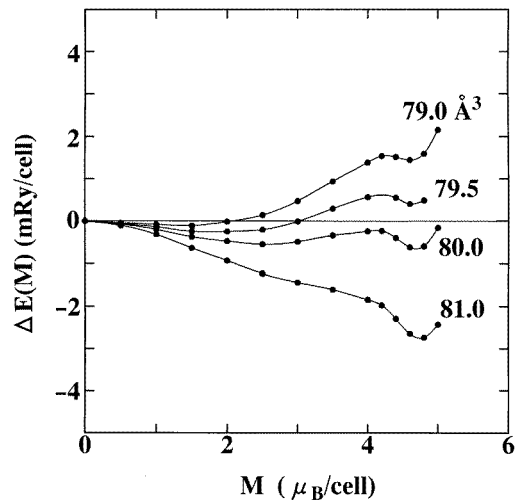


Figure 9. $\Delta E(M)$ calculated for $\text{Y}(\text{Co}_{0.6}\text{Ni}_{0.4})_5$ at various unit-cell volumes.

is proportional to the inverse of the high-field susceptibility.

In figure 8, the local moments $m_{\text{Co}(2c)}$, $m_{\text{Co}(3g)}$ and m_{Y} of Co at 2c and 3g sites and Y for YCo_5 are shown as functions of the total moment M for various values of V , by open squares, triangles and circles, respectively. There are only small differences between them for different values of V . From figure 8, it can be seen that the local moments $m_{\text{Co}(2c)}$ and $m_{\text{Co}(3g)}$ are almost the same as each other for the HMS with $M \geq 6.5 \mu_{\text{B}}/\text{cell}$ at $x = 0.0$ in figure 4. However, for the LMS with $M \leq 3.5 \mu_{\text{B}}/\text{cell}$, $m_{\text{Co}(3g)}$ is rather smaller than $m_{\text{Co}(2c)}$. A small negative moment is obtained at the Y site.

Figures 9, 10 and 11 show the $\Delta E(M)$ calculated for $x = 0.4, 0.5$ and 0.6 in $\text{Y}(\text{Co}_{1-x}\text{Ni}_x)_5$, respectively. The numbers shown on the curves denote the values of V in \AA^3 . In figure 9 a

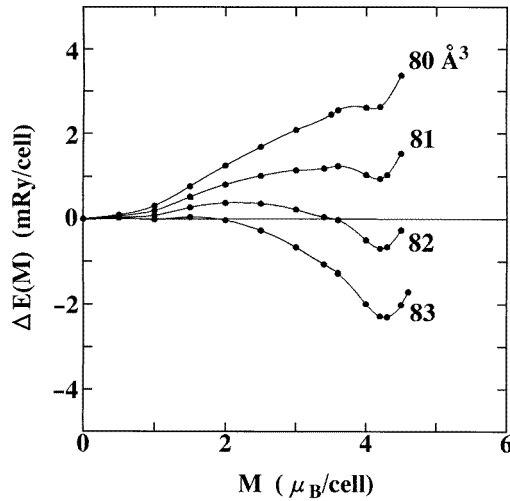


Figure 10. $\Delta E(M)$ calculated for $\text{Y}(\text{Co}_{0.5}\text{Ni}_{0.5})_5$ at various unit-cell volumes.

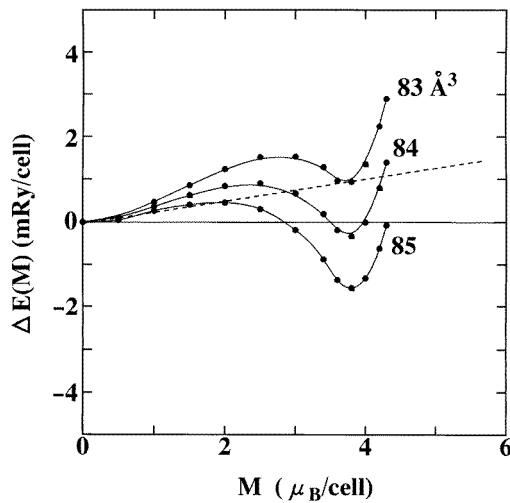


Figure 11. $\Delta E(M)$ calculated for $\text{Y}(\text{Co}_{0.4}\text{Ni}_{0.6})_5$ at various unit-cell volumes. The broken line denotes the tangential line for $\Delta E(M)$ at 83\AA^3 .

broad minimum of $\Delta E(M)$ for $V = 80 \text{ \AA}^3$ can be seen near $M = 0.28 \mu_B/\text{cell}$, which is the LMS at $x = 0.40$ in figure 4. However, such a broad minimum disappears in figures 10 and 11 and the paramagnetic state is stabilized at these concentrations of Ni. This is expected when the position of E_F lies near the minimum of the DOS.

Above the critical concentration of Ni shown in figures 5 and 6, the minimum value of $\Delta E(M)$ at large M becomes positive. In this case, the MT takes place from the paramagnetic state to the ferromagnetic one as a result of the applied magnetic field. The present MT is caused by the shape of the local DOS of the virtual 3d atom of Co and Ni at the 3g site near E_F , as the position of E_F lies near the minimum of the DOS. The critical field of the MT is estimated as the slope of the tangential line, as shown by the broken line in figure 11. The critical field is very sensitive to the unit-cell volume and it is hard to estimate. For instance, the critical field is about 60 T for $V = 83 \text{ \AA}^3$ at $x = 0.6$, while the critical field becomes negative for $V = 84 \text{ \AA}^3$; that is, it is still ferromagnetic. Moreover, in this paper, we have not taken into account the effect of the magneto-elastic energy—that is, of the magnetic pressure. The critical field for the MT becomes small when the magneto-volume coupling is taken into account [16]. Therefore, the critical field cannot be estimated quantitatively from the present calculations.

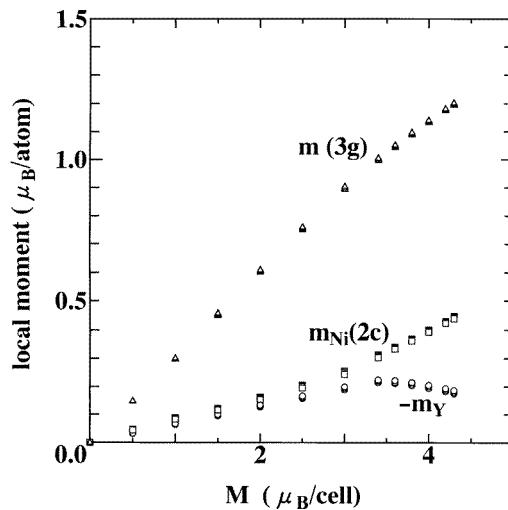


Figure 12. Calculated local moments $m(3g)$, $m_{Ni}(2c)$ and m_Y of the virtual 3d atom of Co and Ni at the 3g site, the 2c-site Ni and the Y atoms in $Y(\text{Co}_{0.4}\text{Ni}_{0.6})_5$, respectively, as functions of the total moment M .

The open triangles, squares and circles in figure 12 show the calculated local moments $m(3g)$, $m_{Ni}(2c)$ and m_Y , of the virtual 3d atom at the 3g site, the 2c-site Ni atom and the Y atom, respectively, as functions of the total moment M for $x = 0.6$. Small induced moments are seen on the 2c-site Ni atom and on the Y atom, due to the hybridization between the 3d states of the virtual 3d atom at the 3g site and that of Ni at the 2c site or the 4d states of Y.

4. Conclusions and discussion

In this paper, we have calculated the electronic structure of the pseudo-binary compound $Y(\text{Co}, \text{Ni})_5$, by taking into account the preferred site of Ni. The bulk moment has been shown to disappear abruptly near 60% Ni concentration. Above the critical concentration of Ni, the

MT from the paramagnetic to the ferromagnetic state has been shown to take place. These results are consistent with the recently observed ones [5].

The anomalous magnetic behaviours of $Y(\text{Co}_{1-x}\text{Ni}_x)_5$ near $x = 0.6$ are caused by the detailed shape of the DOS curve of the virtual 3d atom of Co and Ni at the 3g site near E_F . As shown in figure 3, E_F at $x = 0.6$ lies near a broad minimum of the local DOS of the virtual 3d atom at the 3g site. In such a case the magnetic energy $\Delta E(M)$ has a double minimum at a finite M and at $M = 0$. When the minimum of $\Delta E(M)$ at $M = 0$ is lower than that at finite M —say, the case of the curve labelled 83 Å in figure 11—the MT occurs at a certain magnetic field. In this way the anomalous magnetic behaviours observed for $Y(\text{Co}, \text{Ni})_5$ near the critical concentration can be understood on the basis of the DOS calculated in the present paper, where the preferred site of Ni is taken into account.

Very recently, a large negative magnetoresistance has been observed at 4.2 K for $Y(\text{Co}_{1-x}\text{Ni}_x)_5$ near $x = 0.65$ [17]. This observed result will be caused by the MT of the 3g-site atom by the magnetic field. In the actual compound, some 3g-site atoms will be in the HMS even at $H = 0$ above the critical concentration, due to the atomic environment of Co and Ni at the 3g site, and others are in the LMS. As seen in figure 1, in fact, a small moment even at $H = 0$ is observed for $x = 0.65$. Thus the compound will show a large residual resistance just above the critical concentration, because of the coexistence of the magnetic and nonmagnetic atoms at the 3g site when there is no magnetic field. In fact, an extremely large resistivity is observed when there is no magnetic field for the samples with high quality [17].

When an external magnetic field higher than the critical field of the MT is applied, most of the 3g-site atoms will be in the HMS and, then, the residual resistance will become small. Therefore, the observed large negative magnetoresistance near the critical concentration for $Y(\text{Co}, \text{Ni})_5$ is possibly attributable to the present MT at the 3g-site atom. However, the total magnetic moment, in this case, should become much larger than the one observed at $H = 40$ T, when most of the 3g-site atoms are in the HMS, as has been postulated. This discrepancy between the calculated and observed bulk moments near the critical concentration will be due to the present treatment of 3g-site atoms as virtual atoms with the averaged atomic number of Co and Ni, as mentioned in section 2. Further quantitative studies, taking into account the alloying effects, on the concentration dependence of the induced moments for $Y(\text{Co}, \text{Ni})_5$ are left to future work.

Acknowledgments

We are very grateful to Professor E Gratz for informing us of observed results on the magnetoresistance for $Y(\text{Co}, \text{Ni})_5$ before publication, and also for valuable discussion.

References

- [1] Franse J J M and Radwanski R J 1993 *Handbook of Magnetic Materials* vol 7, ed K H J Buschow (Amsterdam: Elsevier) p 307
- [2] Givord D, Laforest J and Lemaire R 1979 *J. Appl. Phys.* **50** 7489
- [3] Nordström L, Johansson B, Eriksson O and Brooks M S S 1990 *Phys. Rev. B* **42** 8367
- [4] Bartashevich M I, Goto T, Korolyov A V and Ermolenko A S 1996 *J. Magn. Magn. Mater.* **163** 199
- [5] Ishikawa F, Yamaguchi M, Mitamura H and Goto T 1998 unpublished
- [6] Malik S K, Arlinghaus F J and Wallace W E 1977 *Phys. Rev. B* **16** 1242
- [7] Nordström L, Eriksson O, Brooks M S S and Johansson B 1990 *Phys. Rev. B* **41** 9111
- [8] Nordström L, Brooks M S S and Johansson B 1992 *J. Phys.: Condens. Matter* **4** 3261
- [9] Kitagawa I, Terao K, Aoki M and Yamada H 1997 *J. Phys.: Condens. Matter* **9** 231
- [10] Yamaguchi M and Asano S 1997 *J. Magn. Magn. Mater.* **168** 161

- [11] Chuang Y C, Wu C H and Chang Y C 1982 *J. Less-Common Met.* **84** 201
- [12] Deportes J, Givord D, Schweizer J and Tasset F 1976 *IEEE Trans. Magn.* **12** 1000
- [13] Andreyev A V, Deryagin A V and Zadvorkin S M 1985 *J. Met. Metall.* **59** 116
- [14] Buschow K H J, Brouha M, Biesterbos J W M and Dirks A G 1977 *Physica B* **91** 261
- [15] Moruzzi V L, Marcus P W, Schwarz K and Mohn P 1986 *Phys. Rev. B* **34** 1784
- [16] Yamada H and Shimizu M 1989 *Physica B* **161** 179
- [17] Gratz E, Lindbaum A, Markosyan A S and Milnera M 1998 *J. Magn. Magn. Mater.* **184** 372